

Contents lists available at ScienceDirect

I.WT

journal homepage: www.elsevier.com/locate/lwt





Comparative studies on enhancing pea protein extraction recovery rates and structural integrity using ultrasonic and hydrodynamic cavitation technologies

Jiafei Tang ^{a, b}, Xianglu Zhu ^{a, b}, Gaoya Dong ^{a, b}, Shay Hannon ^a, Hugo M. Santos ^c, Da-Wen Sun ^{b, *}, Brijesh K. Tiwari ^a

ARTICLE INFO

Keywords: Ultrasonic cavitation Hydrodynamic cavitation Pea protein extraction Protein recovery rate Protein structure changes

ABSTRACT

This study explored the efficacy of various cavitation technologies, including ultrasonic bath (USB), ultrasonic plate (US-plate), ultrasonic probe (US-probe), and hydrodynamic cavitation (HDC), in extracting proteins from peas. US-probe showed the highest protein recovery rate (52.53 g/hg protein in pea powder) among all lab-scale cavitation equipment while HDC demonstrated significant potential for scaling up, notably improving both the purity (80.35 g/hg dried precipitate) and recovery rate (56.85 g/hg) of pea protein isolate (PPI) compared to conventional extraction (CE). SDS-PAGE, LC-MS/MS, FTIR and Fluorescence analysis were used to analyse the impact of these cavitation technologies on the structures of pea protein. The results confirmed that cavitation preserved PPI's primary structure while altering its secondary and tertiary structures, particularly under US-probe treatment, which significantly unfolded proteins. The SEM results revealed a marked reduction in protein bodies adhering to starch granules in residues from US-probe and HDC treatments compared to CE, correlating with their higher protein recovery rates.

1. Introduction

With the increasing global emphasis on sustainable food sources, plant-based proteins are emerging as pivotal alternatives to traditional animal-derived proteins. Pea protein, in particular, is gathering wide-spread attention for its superior nutritional profile, inherent gluten-free nature, cost-efficiency, and eco-friendly attributes (Wang, Zhang, & Xu, 2020). Its rich amino acid profile, hypoallergenic properties, wide availability, and non-GMO status make it an increasingly popular choice in the food industry (Yan, Zhao, & Xu, 2024).

Traditional methods for extracting pea protein include alkali extraction/acid precipitation, salt extraction/dialysis, and micellar precipitation. Among these, due to considerations of operational ease and production costs, alkali extraction/acid precipitation is the most commonly employed technique (Wang, Zhang, Xu, & Ma, 2020). However, the lower extraction efficiency and quality of pea protein obtained

through alkali extraction have prompted the development of new strategies to enhance extraction rates, where cavitation technologies have garnered widespread interest due to their relatively high energy efficiency and protein yield (Ochoa-Rivas, Nava-Valdez, & Serna-Saldívar, 2017; Zhang, Zhu, & Sun, 2018). Cavitation can be categorized into four primary types based on its generation mechanism: acoustic, hydrodynamic, optical and particle cavitation. In the realm of food processing, acoustic and hydrodynamic cavitations are particularly favored due to their operational feasibility and potential to enhance the quality and yield of food products (Asaithambi, Singha, & Dwivedi, 2019). Cavitation is a phenomenon that involves the formation, growth, and rapid collapse of bubbles, which can manifest as hydrodynamic cavitation (HDC) caused by pressure fluctuations (Sun et al., 2022) or as ultrasonic cavitation induced by high-frequency sound waves (Bhargava, Mor, & Kumar, 2021; Kiani, Sun, & Zhang, 2012). The implosion of these cavitation bubbles generates various effects including extreme

E-mail address: dawen.sun@ucd.ie (D.-W. Sun).

URL: http://www.ucd.ie/refrig, http://www.ucd.ie/sun (D.-W. Sun).

a Teagasc Food Research Centre, Ashtown, Dublin, Ireland

^b Food Refrigeration and Computerised Food Technology (FRCFT), School of Biosystems and Food Engineering, University College Dublin, National University of Ireland, Belfield, Dublin 4, Ireland

^c REQUIMTE-CQFB, Faculdade de Ciências e Tecnologia, Universidade NOVA de Lisboa, Caparica, Portugal

^{*} Corresponding author.

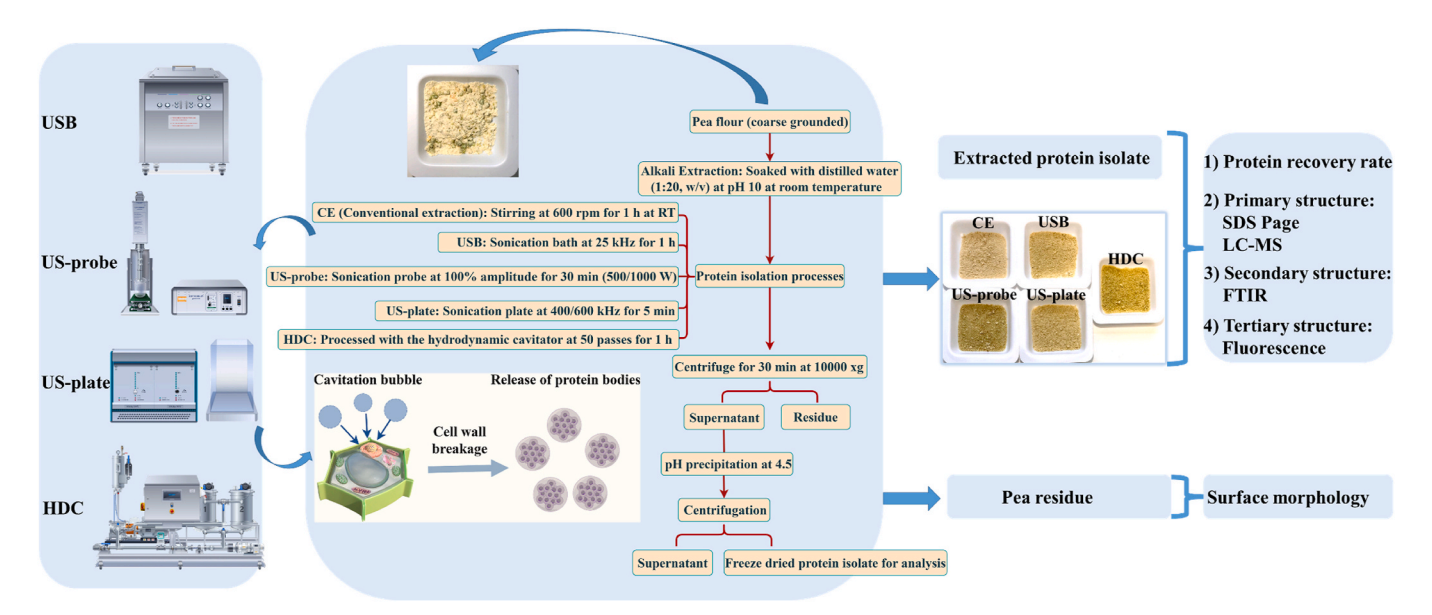


Fig. 1. Graphical abstract of pea protein extraction (By Figdraw). CE: Conventional method, USB: Ultrasonic bath, US-probe: Ultrasonic probe, US-plate: Ultrasonic plate, and HDC: Hydrodynamic cavitation.

temperatures, pressures, shear forces, shock waves, turbulence, and reactive radicals, leading to significant chemical and physical transformations (Li et al., 2020; Tang, Zhu, & Jambrak, 2023; Esua, Sun, Cheng, Wang, & Chen, 2022; Kiani, Sun, & Zhang, 2013; Zhu, Chen, Zhou, & Sun, 2018; Zhu, Sun, Zhang, Li, & Cheng, 2018). Such mechanisms are effective in mechanically and thermally disrupting plant cell walls (Esua, Cheng, & Sun, 2021b), facilitating the release of bioactive compounds into the solvent (Yusoff, Taher, & Rahmat, 2022).

The development of cavitation technology for protein extraction is garnering significant interest due to its promising applications in enhancing safety and offering nutraceutical benefits (Kamal, Ali, & Manickam, 2022). Ultrasonic-assisted extraction (UAE) is notably effective for extracting proteins and bioactive compounds from materials with tough or intricate cell structures (Das et al., 2023). Under specific conditions at solid/liquid ratio of 1:11.5 g:mL, pH 9.6, 13.5 min extraction time and 33.7% ultrasonic amplitude, the extraction efficiency of pea protein isolate (PPI) reached 82.6 g/hg (Wang et al., 2020). Other studies also revealed enhancements in the extraction rate, protein concentration, and yield of peas through ultrasonic treatment (Youshanlouei, Kiani, & Mousavi, 2022). In addition, HDC extraction presents a viable alternative to ultrasonic cavitation for pilot-scale operations due to its low energy consumption and processing consistency (Tang, Zhu, Jambrak, Sun, & Tiwari, 2023). HDC reactors include common types such as orifice type, venturi type, rotating type, and vortex-based type. Beyond these, technologies such as high-pressure homogenizers, microfluidizers, and swirling jet cavitation reactors can also generate hydrodynamic cavitation (Wang, Su, & Zhang, 2021). Research indicated that High-Pressure Homogenisation (HPH) treatments could significantly enhance protein extraction rates, achieving up to 82 g/hg from soy slurry in a single pass under a pressure of 100 MPa (Preece, Hooshyar, & Krijgsman, 2017). Comparative analyses between laboratory-scale UAE and pilot-scale HDC (20 passes) had shown that HDC markedly increased faba bean protein recovery rate of 46 g/hg (Das et al., 2023).

Moreover, cavitation technology not only enhances extraction yields but also modifies the interaction dynamics among protein molecules – such as hydrophobic and electrostatic interactions, hydrogen bonding, disulfide bridges, and Van Der Waals forces – thereby altering the structural configuration (primary, secondary, tertiary and quaternary) of food proteins (Venkateswara Rao, CK, & Rawson, 2023). This has crucial implications for the functional application of plant proteins in

food products. Many papers have reported that high-intensity ultrasound could cause changes in the secondary and tertiary structures of pea protein (Cheng & Cui, 2021; Gao, Rao, & Chen, 2022; Gao, Zha, & Yang, 2022). In addition, there was also a review article that evaluated hydrodynamic cavitation generated by dynamic high-pressure treatment (DHPT) changing the structure of plant protein macromolecules, thereby changing their physicochemical, functional and physiological properties (Sahil, Madhumita, & Prabhakar, 2022).

The innovation of our research lies in the comprehensive application and optimization of these cavitation technologies, specifically designed for pea protein extraction. Distinct from prior research that primarily focused on ultrasonic cavitation extraction of peas for small-scale laboratory applications or on HPH from different sources such as soybeans, our study pioneers the use of HDC for pea protein, a topic that has received little attention in existing literature. Moreover, our research methodically assesses and contrasts ultrasonic extraction and HDC at both laboratory and pilot scales under standardized conditions. This dual-scale evaluation not only measures the cavitation's effectiveness in enhancing the yield and quality of pea protein but also examines their influence on the protein's structural integrity – essential aspects for its functional use in food products. Overall, this study highlights the potential of cavitation technology to revolutionize pea protein extraction, advancing plant protein processing and supporting the growing demand for sustainable plant protein sources.

2. Materials and methods

2.1. Materials and chemicals

Pea grains (*Pisum sativum* L.) used in this study were obtained at the Oak Park experimental research farm in Carlow, Ireland. The grains (moisture content of 10.68 \pm 0.04 g/hg) were kept in cool and dry conditions until further use. The grains were milled to fine powder in a grinder (Robot Coupe Robot Cook Cutter Mixer 43001 R, Ireland). All samples were stored at 4 $^{\circ}$ C prior to further processing. All reagents used were of analytical grade and obtained from Sigma, Ireland. Distilled water was used for all protein extractions and analysis experiments.

2.2. Pea protein extraction process

The graphical abstract of pea protein extraction and analysis can be

J. Tang et al. LWT 200 (2024) 116130

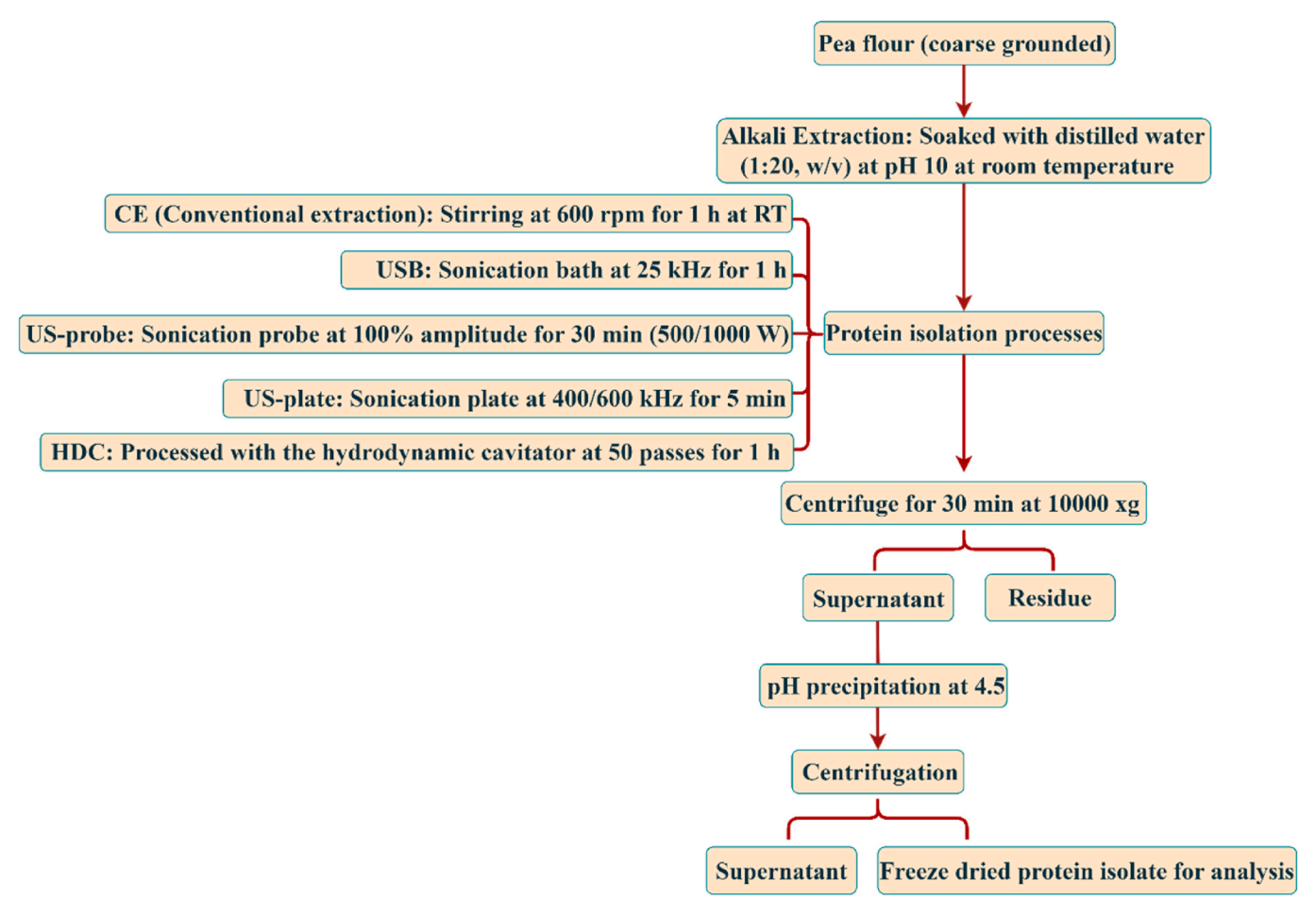


Fig. 2. Schematic flow chart of pea protein extraction processes employed.

 Table 1

 Proximate compositions based on dry matter of pea flour.

Proximate compositions	Concentration (g/hg)		
Protein	19.40 ± 0.64		
Carbohydrate	66.09 ± 0.25		
Moisture	10.68 ± 0.03		
Lipid	1.17 ± 0.10		
Ash	2.66 ± 0.26		

Note: Means \pm standard deviation of replicate samples.

seen as Fig. 1. The schematic flow chart of pea protein isolation processes is shown in Fig. 2. While, conventional extraction (CE), ultrasound bath (USB), ultrasound probe (US-probe) and ultrasound plate (US-plate) extraction were carried out at lab scale using 50 g of pea flour, hydrodynamic cavitation (HDC) was up-scaled using 1 kg of the pea flour. The proximate compositions of the pea flour are shown in Table 1. For extraction procedures, 50/1000 g pea flour was dispersed in 1000 mL/20 L distilled water (1:20 g/mL), respectively, and then pH was adjusted to pH 10 using 1 mol/L NaOH.

2.2.1. Conventional extraction (CE)

CE was carried out as control treatments modified from (Tanger, Engel, & Kulozik, 2020) and treated with 600 rpm stirring for 1 h using a Firex crucifix mixer (Sedico, Italy) at room temperature.

2.2.2. Ultrasound bath extraction (USB)

The ultrasound bath system named Elmasonic xtra ST (25/45 kHz, Elma, Germany) is a floor-mounted ultrasonic device, consisting of a

single tank. USB was performed while the beaker containing the sample solution was placed inside the tank filled with deionized water and treated with ultrasound at 25 kHz for 1 h at room temperature.

2.2.3. Ultrasound probe extraction (US-probe)

The set-up of the probe system (1000 W, UIP 1000hdT, Hielscher, Germany) consists of a UIP 1000 hdT generator and transducer equipped with a 13 mm diameter probe at 20 kHz. The trial showed that 1 h of US-probe could lead to a higher solution temperature. Therefore, in order to reduce the impact of high temperature on extracted protein, in actual experiments, US-probe was conducted using two probe systems (500/ $1000~\rm W$, UIP $500/1000\rm hdT$) for 30 min, respectively. The probe was submerged 30 mm under the water surface for extraction at 100% amplitude.

2.2.4. Ultrasound plate extraction (US-plate)

SONOSYS® Ultrasonic/Megasonic Submersible System (600 kHz, 500 W, SONOSYS, Germany) includes an ultrasonic generator and a tank with a fully encapsulated submersible transducer mounted on the bottom. The trial showed that the sample solution would boil within 8 min of US-plate treatment, therefore, in actual experiments, the sample solution was directly poured into the tank with ultrasonic treatment (100% amplitude, 5 min) at $400/600 \, \text{kHz}$, respectively.

2.2.5. Hydrodynamic extraction (HDC)

The customized HDC-assisted extraction employed a reactor (CaviMax, UK), which consists of a hydraulic pump, a substrate pump, a cavitator pump as well as two storage tanks of 50 L volume. An amount of 1 kg of pea flour was dispersed in 20 L of distilled water (pH 10) in the

storage tank. Then the mixed sample was processed by using the hydrodynamic cavitator, which was operated at a pump speed of 50 Hz, a rotacav speed of 50 Hz and a flow rate of 800 L/h. It is counted as one pass when all the solution passes once through the hydrodynamic pump. Fifty passes were treated with around 1 h. Samples were then stored at 4 $^{\circ}\mathrm{C}$ for further study.

2.3. Collection and recovery of extracted protein

After extraction of protein in solution, the pea residue was separated from the extract solution by centrifugation at $10000 \times g$ for 20 min (Sorvall LYNX 6000 super-speed centrifuge, Thermo Fisher Scientific, Dublin, Ireland). For all treatments, the supernatant solution underwent pea protein isoelectric point (IEP) at pH 4.5, followed by the precipitated protein collection through centrifugation and finally freeze drying to obtain the pea protein isolates (PPI).

The protein content of the extract/isolates was measured in a nitrogen analyser (FP-328 Leco Instrument, Leco Corporation, USA) based on the Dumas principle (method 968.06 (AOAC, 1995), and conversion factor 6.25), and extraction efficiency was also evaluated by calculating the protein recovery rate (g/hg) and extraction yield (g/hg) as described below (Das et al., 2023; Wen et al., 2021):

MWCO), with a subsequent addition of 200 μL of 2 g/dL SDS in 25 mM Ammonium Bicarbonate (AmBic). After centrifugation at 14,000×g for 20 min, proteins were washed with 200 μL of 8 M urea in 25 mM AmBic.

Proteins were reduced using 200 μL of 50 mM dithiothreitol (DTT) in 8 M urea and 25 mM AmBic, followed by ultrasonic treatment. Alkylation was carried out with 100 μL of 50 mM iodoacetamide (IAA) in 8 M urea and 25 mM AmBic, accelerated by ultrasonic treatment. Subsequently, 100 μL of 1:30 (mL/mL) trypsin in 12.5 mM AmBic was added, and protein digestion was processed using ultrasonic treatment. Peptides were dried and stored at $-20~^{\circ} C$ until Nano-LCMS/MS analysis.

The analysis involved an EASY nLC II coupled to an Impact HD (Bruker Daltonics) with a CaptiveSpray nanoBooster, as described previously (Carvalho, Capelo-Martínez, & Lodeiro, 2019; Carvalho, Capelo-Martinez, Lodeiro, Wisniewski, & Santos, 2020). Peptides were resuspended in 3 g/dL acetonitrile with 0.1 g/dL formic acid, homogenized, and loaded onto an EASY-nLC II. Chromatographic separation employed a linear gradient of 0–35 g/dL buffer B over 90 min. MS acquisition was set to cycles of MS followed by MS/MS, with active exclusion. Spectra were acquired in the range of 150–2200 m/z.

Relative label-free quantification utilized MaxQuant software V2.2.0.0. Raw files were processed with default parameters (Cox & Mann, 2008; Tyanova et al., 2015), and database searches were performed using the Andromeda search engine (Cox et al., 2011). Data

Protein recovery rate
$$(g/hg) = \frac{\text{Protein content of precipitate x amount of dried precipitate obtained } (g)}{\text{Protein content in pea samples used for extraction } (g)} \times 100$$

 $\begin{aligned} &\text{Extraction yield } (g/hg) \! = \! \frac{\text{Amount of dried precipitate obtained } (g)}{\text{Weight of raw material used for protein extraction } (g)} \\ &\times 100 \end{aligned}$

(2)

2.4. Analysis of pea protein isolates (PPI)

2.4.1. Molecular weight distribution

The evaluation of molecular weight distribution was conducted by sodium dodecyl sulfate-polyacrylamide gel electrophoresis (SDS-PAGE) with modifications (Arteaga, Guardia, & Muranyi, 2020). In general, aliquots ranging from 4.98 to 6.07 mg of PPI were blended with 0.5 mL of distilled water and 0.5 mL of Laemmli 2 × Concentrate to attain a protein concentration of 4 mg/mL. Following a 15-min heat treatment at 90 °C, the samples underwent centrifugation at 10,000 rpm for 10 min using the Eppendorf® Centrifuge 5430/5430 R (Merck, Ireland). Subsequently, 15 µL aliquot was loaded into the gel wells of Bio-Rad 4–20% Criterion™ TGX Stain-Free™ Protein Gels, immersed in running buffer created by diluting (1:10 mL/mL) the 10× Tris/Glycine Buffer. The Broad Range Unstained Standard (Bio-Rad, Germany) served as the molecular weight marker. Gel electrophoresis was conducted for 1.5 h at 5 W and room temperature. Gel staining was performed using Coomassie Brilliant Blue R-250 Staining solution. Finally, gel images were acquired using the GS-800 Calibrated Densitometer (Bio-Rad, Germany). The entire SDS-PAGE procedure was duplicated for validation purposes.

2.4.2. Liquid chromatography with tandem mass spectrometry (LC-MS/MS)

Protein digestion utilized the Filter-aided sample preparation method (FASP) following the procedure by Wiśniewski (2019), Wiśniewski, Zougman, and Nagaraj (2009), with modifications from Carvalho, Capelo-Martínez, and Lodeiro (2020). Briefly, 50 µg of protein was loaded into a Vivaspin 500 centrifugal concentrator (10,000 Da

processing was performed using Perseus with default settings (Tyanova et al., 2016). Statistical analysis utilized a Multiple-sample Anova test with permutation-based FDR.

2.4.3. Fluorescence analysis

Emission spectra were recorded using a Horiba-Jobin-Yvon Fluoromax-4 spectrofluorometer at 20 °C and were conducted according to the methods (Esua, Sun, Cheng, Wang, & Lv, 2022) with modifications.. The pea protein solution was prepared in phosphate buffer saline (PBS) and pH 7.4. Insoluble materials were spun down by centrifugation at $10000\times g$ for 10 min. Clear supernatants were further used for total protein quantification by Bradford assay. For Fluorescence emission analysis, protein concentrations were adjusted to 0.1 mg/mL with PBS and pH 7.4. The fluorescence was excited at 295 nm, and the emission was recorded from 320 to 400 nm. The fluorescence of the whole cell lysates diluted in 8 M urea containing 10 mM Tris-HCl, pH 8.5, was measured in standard cuvettes ($10\times 10~\text{mm}^2$), whereas the measurements of peptide digests were conducted in a HELMA 1 cm light path quartz cell.

2.4.4. Fourier transform infrared spectrometer (FTIR) measurement and multivariate data analysis

Sample (0.5 g) was placed on the surface of a diamond crystal attenuated total reflectance (ATR) accessory (iD7 ATR, Thermo Scientific, Madison, WI, USA), and spectral measurements were carried out using an FTIR (NicoletTM iS5, Thermo Scientific, Madison, WI, USA). Single-beam reflectance spectra were collected and converted into absorbance spectra in the wavelength range of 450–4000 cm $^{-1}$ with a resolution of 2 cm $^{-1}$. Air blank background calibration was carried out before each measurement. 64 scans were performed on each measurement to acquire the averaged spectral data. Spectral data acquisition was managed using the supplied OMNIC software v 9.2.98 (Thermo Fisher Scientific Inc., USA). Each sample was measured in quadruplicate at two different surface areas.

Table 2The effect of cavitation technologies on the production of pea protein.

Extraction technology	Protein content (g/hg)	Extraction yield (g/hg)	Protein recovery rate (g/hg)
HDC	80.35 ± 2.18^a	_	56.85 ± 4.59^a
USB	$78.76 \pm 1.47^{a,b}$	11.98 ± 0.20^{a}	$46.72 \pm 0.10^{\mathrm{b}}$
US-probe 1000	$74.97 \pm 1.99^{a,b}$	14.15 ± 0.33^a	$52.53 \pm 0.19^{\mathrm{a,b}}$
US-plate 400	$74.93 \pm 0.34^{a,b}$	12.87 ± 0.01^{a}	47.76 ± 0.16^{b}
US-probe 500	$72.83 \pm 0.47^{a,b}$	14.22 ± 0.71^{a}	$51.29 \pm 2.22^{a,b}$
US-plate 600	$72.73 \pm 2.32^{a,b}$	12.98 ± 0.71^{a}	$46.72 \pm 1.06^{\rm b}$
CE	65.94 ± 7.59^{b}	13.94 ± 1.33^a	$45.28 \pm 0.90^{\rm b}$

Note: All data are the mean \pm standard deviation of three replicates. Means followed by different letters (a, b) within the same column are significantly different (p < 0.05) from each other. The units in the table are as follows: protein content (g/100 g dried precipitate), extraction yield (g/100 g pea powder), and protein recovery rate (g/100 g protein in pea powder). HDC: hydrodynamic cavitation 50 passes, USB: ultrasonic bath, US-probe 1000: ultrasonic probe with 1000 W, US-plate 400: ultrasonic plate with 400 kHz, US-probe 500: ultrasonic probe with 500 W, US-plate 600: ultrasonic plate with 600 kHz, and CE: Conventional method.

2.4.5. Scanning electron microscopy (SEM)

The estimation of morphological changes in the pea flour residues was carried out by SEM. Sample preparation for SEM was modified as described by Zhu et al. (2022) and Esua, Cheng, and Sun (2021a). The samples were rehydrated, then fixed in 2.5 g/dL glutaraldehyde mixture buffered with 0.1 M phosphate buffer (pH 7.4) for 6 h at 4 °C, post-fixed in 1 g/dL osmium tetroxide in the same buffer for 1.5 h at 4 °C. After fixation, the samples were dehydrated in graded ethanol (30 g/dL, 50 g/dL, 70 g/dL, 80 g/dL, 90 g/dL, and 100 g/dL). The dried samples were mounted on stubs and then coated with a 5 nm layer of Gold using an Emitech K575X Peltier Cooled Sputter Coating Unit (Quorum Technologies). Sample surfaces were photographed with a scanning electron microscope (Regulus 8230, Hitachi, Japan).

2.5. Statistical analysis

One-way analysis of variance (ANOVA) was used to test for differences in mean values between different treatments, followed by Tukey's

honestly significant differences (HSD) multiple rank test at p < 0.05. The results were shown as mean \pm standard deviation (SD). ANOVA was performed by the Minitab Program for Windows version 18.0 (Minitab, LLC, and State College, PA, USA).

3. Result and discussion

3.1. Protein recovery efficiency

Extant research predominantly utilized alkaline pH solvents for legume protein extraction and recovery, followed by pH adjustment to the protein's isoelectric point in the supernatant to yield a concentrated protein product (Das et al., 2023; Wang et al., 2020). As delineated in Table 2, extraction yield did not significantly differ across all technologies at a 50 g laboratory scale (USB, US-probe 1000, US-probe 500, US-plate 600, US-plate 400, and CE). However, for protein content, all ultrasonic treatments uniformly outperformed the CE (65.94 \pm 7.59 g/hg), achieving up to 78.76 \pm 1.47 g/hg (USB). This enhancement is attributed to ultrasound-induced cavitation, which disrupts cellular structures and molecular bonds, thereby facilitating mass transfer and enhancing protein extraction efficiency (Tang et al., 2023; Youshanlouei, Kiani, Mousavi, & Mousavi, 2022). Regarding recovery rates, both USB and US-plate treatments exhibited slight improvements over the CE (45.28 \pm 0.90 g/hg), at 46.72 \pm 0.10 g/hg and 47.76 \pm 0.16 g/hg, respectively, but the US-probe technique significantly increased this rate to 52.53 ± 0.19 g/hg, demonstrating the highest recovery rate among all ultrasound instruments. In addition, the high-frequency US-plate was deemed inappropriate for plant protein extraction due to its rapid heating effects (boil). Based on the above results, US-probe could be considered the most effective ultrasound technology for extracting pea protein. This aligned with prior findings where high-intensity ultrasound was shown to augment pea protein recovery rates (de Oliveira et al., 2020; Karabulut, Yildiz, & Karaca, 2023; Wang et al., 2020).

Despite its efficacy at a laboratory scale, the US-probe technique faces scale-up challenges, primarily due to inconsistent processing conditions (Bernardi et al., 2021). Hence, HDC presents a viable alternative for pilot-scale exploration in plant protein extraction. Compared

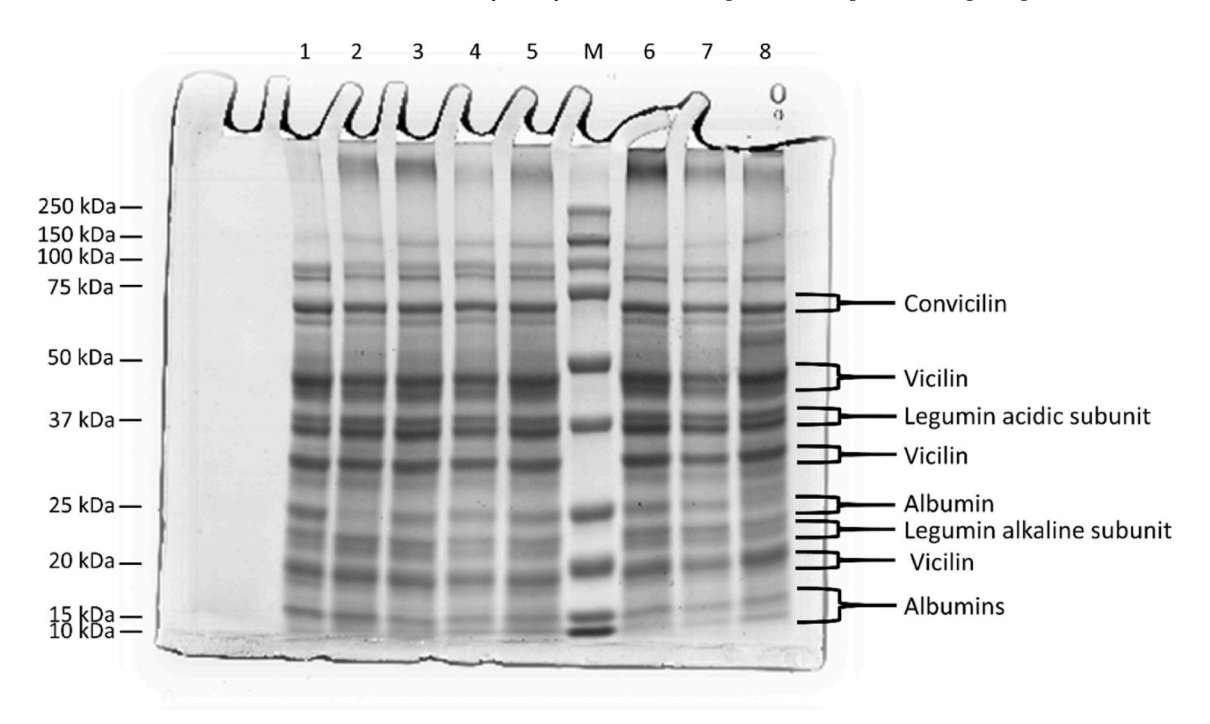


Fig. 3. SDS-PAGE profile of pea protein isolates (PPI) under reducing conditions. Lane M indicates standard protein marker, lane 1: Raw material, lane 2: HDC, lane 3: US-plate 600, lane 4: US-plate 400, lane 5: US-probe 1000, lane 6: US-probe 500, lane 7: USB, lane 8: CE.

Table 3Major proteins identified by mass spectrometry analysis.

Protein type	MW (kDa)	Accession	Protein Name	T: Significant pairs ^a
Legumin	65.6	gi 2314289354	legumin B-like	
	65.6	gi 2314293535	legumin B	CE_US-plate; CE_HDC
	59.3	gi 126161	Legumin A2 (precursor)	US-probe_HDC; US- probe_US-plate; USB_HDC; USB_US- plate; CE_HDC; CE_US-plate
	56.9	gi 126170	Legumin J (precursor)	CE_US-plate; CE_HDC; CE_US- probe
	55.9	gi 2314277731	legumin J-like	•
Vicilin	52.7	gi 2314261201	vicilin-like	
	52.3	gi 2314260297	vicilin-like	
	52.2	gi 2314260286	Vicilin	USB_US-plate
	52.2	gi 2314260279	vicilin-like	
	52.2	gi 2314261444	vicilin-like	US-probe_CE; CE_US-plate; CE_HDC
	14.0	gi 137577	Vicilin, 14 kDa component	USB_HDC; USB_US- probe
Convicilin	72.1	gi 2314279111	Convicilin	CE_US-plate; US- probe_US-plate; USB_US-plate
	66.9	gi 2314279115	Convicilin	USB_HDC; CE_HDC; USB_US-plate; CE_US-plate; CE_US-probe
Albumin	26.2	gi 2314148191	albumin-2	USB_HDC; US- probe_HDC
	13.4	gi 2274067070	Albumin-1 D, variant 2	US-plate_HDC; USB_HDC; US- probe_HDC; CE_HDC; CE_US- plate; CE_USB; CE_US-probe
Lipoxygenase	97.6	gi 2314267718	seed linoleate 9 S- lipoxygenase-3	CE_HDC; CE_US- probe
	97.1	gi 126402	Seed linoleate 9 S- lipoxygenase-2	USB_US-plate; CE_US-plate; CE_US-probe; CE_HDC
	97.0	gi 2314267714	seed linoleate 9 S- lipoxygenase-2	
Heat shock protein	80.1	gi 2314257002	heat shock protein 90-2	

^a Means that A has a significantly higher abundance than B in the case of A_B.

to CE, HDC treatment significantly (p < 0.05) enhanced both protein content (80.35 \pm 2.18 g/hg) and recovery rate (56.85 \pm 4.59 g/hg) of PPI, a result attributed to the efficient extraction capabilities of HDC's cavitation effect. Although HDC's application in pea protein extraction is relatively unexplored, the research on faba bean protein extraction identified HDC as the most effective method, yielding the highest protein recovery rate (~70 g/hg), surpassing both ultrasound (41 g/hg) and CE (32 g/hg) (Das et al., 2023). Thus, HDC holds potential as a scalable cavitation technology for pea protein recovery.

3.2. Protein primary structure analysis: SDS page and LC-MS/MS analysis

Pea protein profiles and primary structures were evaluated using SDS-PAGE and LCMS. Peas are rich in a variety of proteins, mainly including globulin (legumin, vicilin, and convicilin) and albumin. Legumin monomer is formed by the covalent linkage of an acidic subunit (40 kDa) and a basic subunit (20 kDa) via a single disulfide bond. Six of these monomers can be non-covalently linked to form a hexametric protein with a molecular weight between 300 and 400 kDa (Lam, Can Karaca, & Tyler, 2018). Vicilin is a trimer with a molecular weight of 150–170 kDa and its monomeric molecular weight is approximately 47–50 kDa. Convicilin monomer has a molecular weight of approximately 70 kDa and forms trimers of approximately 210 kDa or 290 kDa (including the N-terminal extension) (Lam, Can Karaca, Tyler, & Nickerson, 2018). Albumin is water-soluble, its molecular weight is between 5 and 80 kDa, and its two main protein polypeptides are 25 kDa and 6 kDa.

Fig. 3 shows protein bands with different cavitation treatments under reducing conditions. No 60 kDa band was found in SDS-PAGE under all treatment conditions, but highly abundant 40 kDa and 20 kDa bands were found, which could be associated with the acidic and basic subunits of legumin, respectively (Moll, Salminen, & Seitz, 2023; Youshanlouei et al., 2022). Under reducing conditions, the disulfide bonds between the acidic and basic subunits of legumin monomers were cleaved, releasing them. Table 3 shows the protein sequences and molecular weight obtained for all processing conditions determined by LCMS. Legumin was present in all protein extracts with a high abundance. However, no protein sequences (40 kDa and 20 kDa) were detected in LCMS analysis, which may be attributed to the conditions applied by mass spectrometry being insufficient to cleave all disulfide bonds, allowing the acidic and basic subunits to combine to form the 60 kDa legumin monomer. It was consistent with previous reports (Moll, Salminen, Seitz, Schmitt, & Weiss, 2023). In addition, protein sequences of 59.3 kDa, 56.9 kDa, and 55.9 kDa were also found in all protein extracts and identified as legumin A2 (precursor), legumin J (precursor) and legumin J-like, respectively (Table 3). For legumin A2 (precursor), US-probe and USB contained significantly higher abundance relative to HDC and US-plate, whereas for other legumin all cavitation treatments did not differ significantly (Table 3).

The 47 kDa, 35 kDa and 18 kDa bands were found in high abundance (Fig. 3) and could be associated with the dissociated vicilin trimer protein (Tanger et al., 2020). Under reducing conditions, the vicilin trimer was cleaved to form a large number of vicilin subunits with a molecular weight of 50 kDa, which can correspond to the high abundance of vicilin in the mass spectrometry results (Table 3). At the \sim 47 kDa band (Fig. 3), it could be clearly seen that the abundance of US-probe was the highest among all treatments, which was consistent with LCMS (Table 3). This may be because the US-probe caused a larger cavitation effect, and the shear stress turbulence caused by it destroyed the hydrophobic interaction of the vicilin trimer. The 62 kDa and 67 kDa bands were associated with the convicilin monomer (Fig. 3) and were also detected by mass spectrometry (Table 3). Bands of 25 kDa and below 15 kDa in SDS-PAGE were considered to be water-soluble albumin (Youshanlouei et al., 2022). Compared with Raw material, the albumin bands of other alkaline extraction conditions were obviously weaker, especially in HDC treatment. The literature indicated that alkaline extraction-isoelectric precipitation protein products precipitated at the isoelectric point of globulin (pH 4.5), whereas the isoelectric point of albumin was approximately pH 6, so they remained dissolved during the precipitation step and were discarded (Swanson, 1990).

Overall, by combining the SDS-PAGE and LCMS results, although US-probe showed a slight advantage, all cavitation treatments did not significantly change the protein bands, which means that cavitation could not cause peptide bond breakage and changes in primary structure. Similar results had been reported for pea protein (Gao, Zha, Yang,

J. Tang et al. LWT 200 (2024) 116130

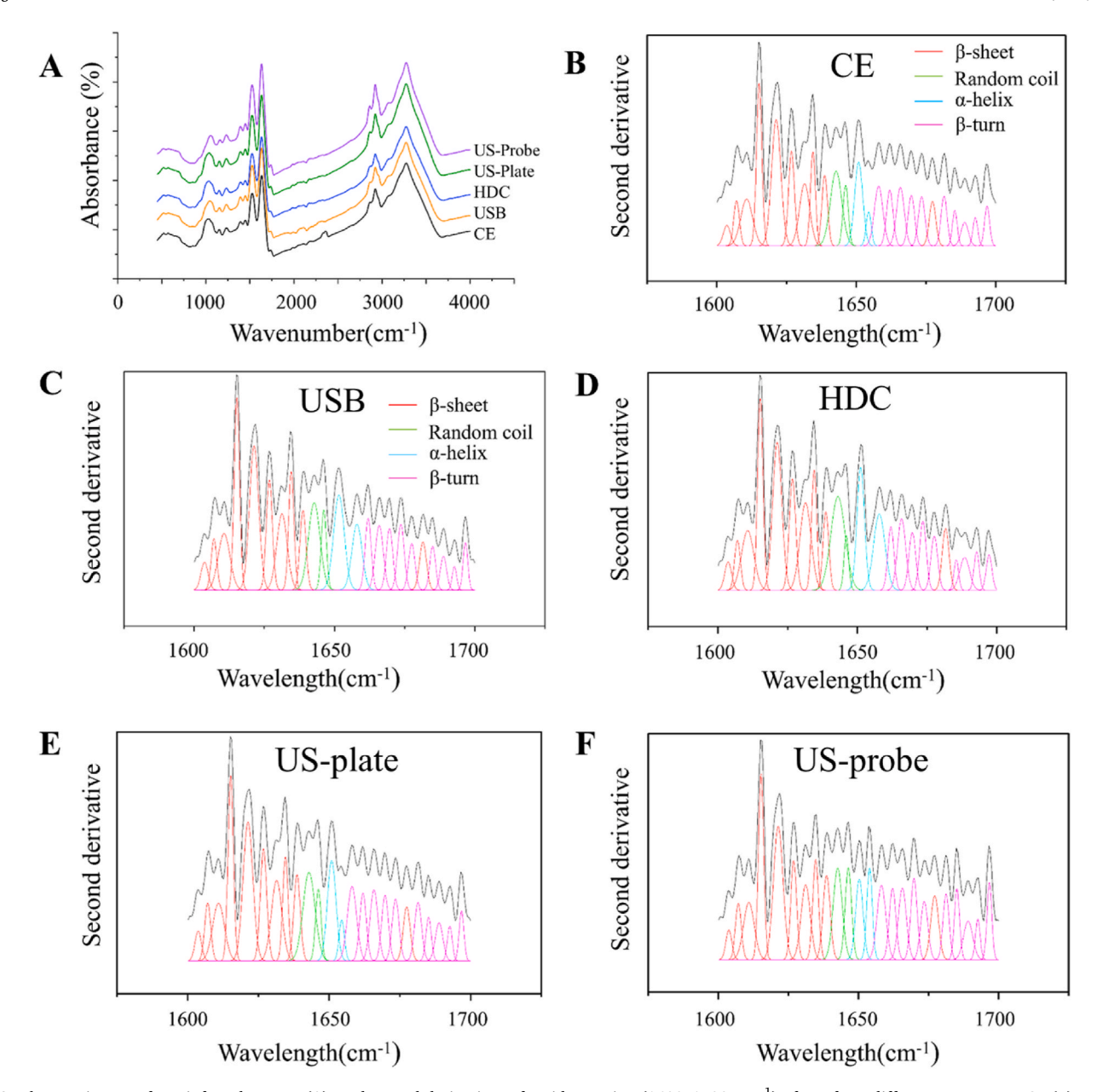


Fig. 4. The Fourier transform infrared spectra (A); and second derivatives of amide I region (1600–1700 cm⁻¹) of PPI from different treatments: CE (B), USB (C), HDC (D), US-plate (E), and US-probe (F).

Table 4Content of secondary structure components of PPI with different treatments.

Treatment	β-sheet/%	random coil/%	α-helix/%	β-turn/%
CE	53.29 ± 0.72^a	11.33 ± 0.12^a	13.91 ± 0.49^a	21.47 ± 0.35^{b}
USB	52.58 ± 0.36^{a}	12.29 ± 0.08^a	12.97 ± 0.07^a	22.16 ± 0.35^b
HDC	52.90 ± 1.12^{a}	12.16 ± 1.13^a	13.37 ± 0.47^a	21.56 ± 1.78^{b}
US-plate	52.66 ± 2.13^a	11.82 ± 0.73^a	12.83 ± 0.98^{a}	22.70 ± 0.42^{b}
US-probe	$47.90 \pm 0.30^{\mathrm{b}}$	12.32 ± 0.17^{a}	11.52 ± 0.32^{a}	28.26 ± 0.15^{a}

Note: All data are the mean \pm standard deviation of three replicates. Means followed by different letters (a, b) within the same column are significantly different (p < 0.05) from each other.

Rao, & Chen, 2022; Mozafarpour, Koocheki, & Nicolai, 2022) and soy protein (Li et al., 2020).

3.3. FTIR analysis of protein secondary structure

FTIR analysis of pea protein extraction via diverse cavitation

technologies yielded crucial insights into the induced structural modifications. The outcomes are presented in Fig. 4 A. The resulting FTIR spectrum exhibited prominent peaks corresponding to specific functional groups within the pea protein. All samples displayed broad peaks in the 3100-3600 cm⁻¹ range due to -OH, -NH, and -CH stretching vibrations, with a sharp peak near 2900 cm⁻¹ attributed to -CH stretching on saturated carbon, in alignment with (Zhang, Kang, & Cheng, 2022). Notably, the region approximately between 1600 and 1700 cm⁻¹ aligned with the amide I band, indicating variations in secondary structure (β -sheet, random coil, α -helix and β -turn) within the pea protein (Gao, Zha, et al., 2022; Shevkani, Singh, & Kaur, 2015). To delve deeper into the influence of various cavitation techniques on protein secondary structure, second-order derivative processing and Gaussian fitting were applied to the obtained FTIR spectra (Fig. 4 B-F, Table 4). Spectral ranges of 1610–1640 cm⁻¹ and 1673-1677 cm⁻¹, 1641-1649 cm⁻¹, and 1649-1657 cm⁻¹ corresponded to β -sheet, random coil, and α -helix structures, respectively. Meanwhile, spectral ranges of 1659–1674 cm⁻¹ and 1681–1696 cm⁻¹ corresponded to β -turn

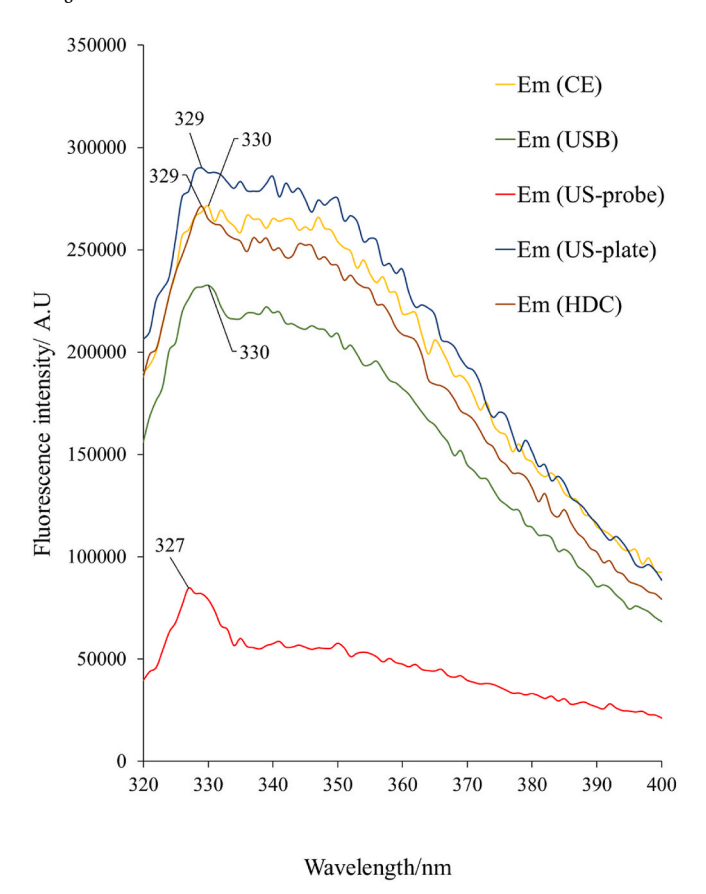


Fig. 5. Intrinsic emission fluorescence of PPI with different treatments of CE, USB, US-probe, US-plate and HDC, respectively. Abbreviations in the figure: Em (emission).

structures (Zhang, Kang, & Cheng, 2022). The peptide chain structure comprising the random coil displayed a non-repetitive and relatively unstable arrangement, whereas the α -helix represented a highly ordered and comparatively stable secondary structure (Zhang, Liu, & Chen, 2022). All cavitation treatments demonstrated slightly higher random coil content and lower α -helix content in comparison to the CE method, indicating that cavitation effects tended to render protein structures more unstable. Beta structures, as stable secondary structures, were connected by varying hydrogen bonding patterns (Cheng & Cui, 2021). In terms of β-sheet content across various extraction methods, the CE method exhibited the highest content at 53.29%, followed by HDC (52.90%), US-plate (52.66%), and USB (52.58%). Additionally, US-probe resulted in a significant reduction in β -sheet content to 47.90% (P < 0.05). This could be attributed to cavitation inducing a greater degree of protein denaturation relative to CE methods, particularly US-probe. Comparative to the CE method, all cavitation techniques displayed slightly higher β-turn content, while the US-probe method showcased a significant increase in β-turn content, reaching 28.26% (P < 0.05). This finding indicated that cavitation led to a rearrangement of hydrogen bonds within the protein molecule, promoting the conversion from β -sheets to β -turns within the β structure. Consistent with previous research (Liu et al., 2023), it was found that sonication caused the α -helix and β -sheet regions of PPI samples to unfold and transform into β-turns and random coils. It is noteworthy that consensus regarding the effect of cavitation treatment on the secondary structure of PPI proteins has not been reached. It was found that PPI treated with pH shift and high intensity ultrasound (HIU) alone exhibited varying degrees of reduction in α -helix and β -turn content compared to native PPI (Zhang, Liu, & Chen, 2022). The research reported that increasing ultrasonic power initially led to an increase followed by a decrease in the β-sheet content of PPI (Gao, Zha, et al., 2022). These diverse outcomes may be attributed to the cavitation technology employed in the respective cases and the differing usage parameters.

3.4. Protein tertiary structure analysis: fluorescence analysis

Fluorescent analysis characterizes spatial conformational changes in proteins caused by exposure to aromatic amino acid residues (Phe, Tyr, and Trp) resulting from protein folding, unfolding, and association (Yang, Zamani, & Liang, 2021). Phe, Tyr, and Trp residues in proteins, especially Trp residue, will fluoresce in a protein folding-dependent manner, so fluorescence analysis can reveal changes in protein tertiary structure (Xiong et al., 2018). The maximum emission wavelength (λ_{max}) is related to the polarity of the microenvironment where the Trp residue is located, while the maximum fluorescence intensity decreases as the exposure of the Trp residue to the aqueous environment increases due to fluorescence quenching (Gao, Zha, et al., 2022).

Fig. 5 shows the spatial conformational changes of PPI under different treatments. Compared with CE treatment, the fluorescence intensity of almost all PPIs decreased after cavitation treatment, except for 5 min US-plate treatment. In addition, US-probe treatment significantly reduced the fluorescence intensity of PPI, because high-intensity ultrasonic probe cavitation led to high denaturation of the protein, which triggered the exposure of the side chains of the fluorescent chromophore residues. Consistent with the current findings, previous studies also reported a decrease in protein fluorescence intensity after high-intensity ultrasonic treatment (Cheng & Cui, 2021; Gao, Rao, & Chen, 2022; Xiong et al., 2018). According to the literature, most of the fluorophore residues are located inside the protein molecule, but different treatment methods will denature part of the protein of the PPI and expose the side chains of the fluorescent chromophore residues, thereby promoting collision quenching, resulting in a decrease in the fluorescence intensity within the protein molecule (Zhang, Kang, & Cheng, 2022; Zhang, Liu, & Chen, 2022). The λ_{max} of CE treatment was 330 nm, while the λ_{max} of US-probe was 327 nm, which meant that λ_{max} was slightly blue-shifted, indicating that the microenvironment of the fluorescent chromophore residues became more non-polar, which may be attributed to cavitation-induced rearrangement of protein molecular chains. In short, the results showed that almost all cavitation treatments reduced fluorescence intensity, confirming changes in the tertiary structure of the protein, which might be caused by the hydrophobic interaction within the protein molecule to be destroyed by the cavitation effect, causing part of the protein to unfold. Among those, the fluorescence intensity of US-probe decreased most obviously.

3.5. SEM analysis of residue surface morphology

Pea cotyledons consist of storage cells rich in starch granules and protein bodies, where the starch granules are embedded in a protein-rich cellular matrix (Pernollet, 1978). After different treatments, pea storage cells ruptured due to cavitation, resulting in most of the protein bodies being extracted, while a large number of starch granules remained in the residue left after protein extraction. To elucidate cell disruption and protein recovery rate caused by different cavitation techniques, the exterior morphology of dried pea residue was visualized by surface morphology (Fig. 6). Notably, large oval or kidney-shaped starch granules were easily observed in all treatments (Fig. 6, red arrow), which was consistent with previously reported findings on different morphologies of market-type peas (Shen, Hou, & Ding, 2016). Compared with other cavitation techniques, CE can only partially disrupt the cell structure, showing that granules of different sizes and roughness were still attached to the starch granules (Fig. 6 A, yellow arrow), which was considered to be the protein body-rich cell matrix (Möller, van der Padt, & van der Goot, 2021). Cavitation technology could relatively completely disentangle starch granules embedded in the cell matrix, which was attributed to the cavitation effects caused by bubble J. Tang et al. LWT 200 (2024) 116130

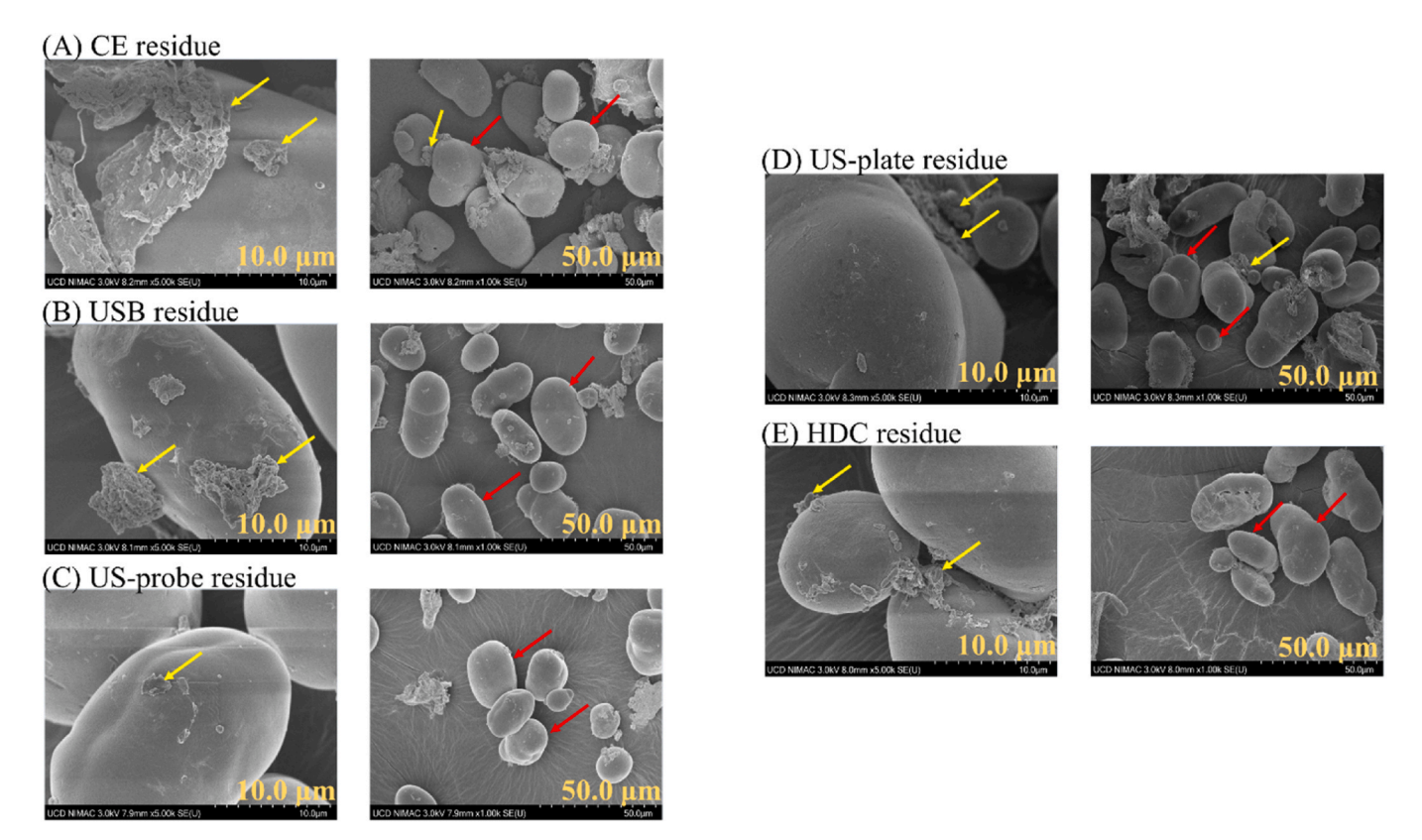


Fig. 6. Scanning electron microscope (SEM) images of pea residue processed from different technologies: (A) CE, (B) USB, (C) US-probe, (D) US-plate and (E) HDC. Red Arrows indicate starch granules and yellow arrows indicate protein-rich cellular matrix. Scale bar in the figure represents 10.0 µm and 50.0 µm, respectively.

oscillation (stable cavitation), bubble implosion (transient cavitation), and shear forces of the liquid flow around the bubble (Tang et al., 2023). It could be found that the degree of starch granule fragmentation was also different between the four cavitation techniques. The remaining residue after HDC (Fig. 6 E) treatment indicated that there was relatively little cell matrix attached to the starch granules. This showed that HDC had a considerable effect in extracting pea protein, and the results also corresponded to its higher protein recovery rate (56.85 g/hg). The US-probe residue showed that the surface attachments of starch granules were obviously the least (Fig. 6 C), and the amount of protein bodies was the least, indicating that it could be the most effective cavitation technology for extracting pea protein, which was consistent with the results of its extraction rate and structural analysis. Previous research also reported similar SEM results (Das et al., 2023). They found that in the extraction of faba bean protein using CE, UAE, HPP (300 MPa), and HDC (20 passes), the UAE residue showed minimal adherence of starch and protein particles with a very low amount of visible protein bodies.

4. Conclusions

In this investigation, we employed a spectrum of cavitation technologies (USB, US-plate, US-probe, and HDC) to extract and recover proteins from peas. The PPIs obtained were subjected to a thorough analysis of their protein recovery rates and structures, encompassing primary, secondary, and tertiary levels. Laboratory-scale experiments revealed that the US-probe technique markedly outperformed other methods in terms of PPI extraction efficiency, while HDC showed promising potential for scaling up, significantly enhancing both the purity and recovery rate of PPI. Detailed SDS-PAGE and LC-MS/MS analysis confirmed the preservation of the primary structure of PPI, indicating that cavitation processes do not compromise peptide bonds. In contrast, FTIR analysis provided insights into alterations in the secondary structure of PPI induced by cavitation. Notably, there was a

transition from α -helixes and β -sheets to random coils and β -turns, a transformation attributable to the disruption and reformation of hydrogen bonds, with changes being most pronounced in the US-probe treatment. Fluorescence spectroscopy analysis further illuminated significant modifications in the tertiary structure of PPI, a result of cavitation disrupting hydrophobic interactions and prompting protein unfolding. Here again, the US-probe method induced the most substantial structural alterations. To elucidate the structural mechanisms of protein extraction and recovery, SEM was employed to examine the residues post-extraction. SEM results showed that protein bodies adhering to starch granules were significantly reduced in residues from US-probe and HDC treatments relative to CE treatment, aligning with their observed higher protein recovery rates. Conclusively, the findings underscore the superiority of the US-probe technique in the context of laboratory-scale ultrasonic cavitation for protein extraction. Additionally, HDC, with its remarkable protein recovery efficacy, emerges as a viable candidate for the upscaling of cavitation technology in the extraction and recovery of proteins on an industrial scale.

CRediT authorship contribution statement

Jiafei Tang: Conceptualization, Investigation, Writing - original draft. Xianglu Zhu: Investigation. Gaoya Dong: Investigation. Shay Hannon: Investigation. Hugo M. Santos: Investigation. Da-Wen Sun: Supervision, Funding acquisition, Writing – review & editing. Brijesh K Tiwari: Supervision, Funding acquisition, Resources, Writing – review & editing.

Declaration of competing interest

The authors declare that they have no known competing financial interests or personal relationships that could have appeared to influence the work reported in this paper.

Data availability

The authors are unable or have chosen not to specify which data has been used.

Acknowledgements

The authors would like to acknowledge the U-Protein project funded by the Irish Department of Agriculture, Food and Marine (DAFM) under the Food Institutional Research Measure (Grant No. 2019PROG702). Jiafei Tang, Xianglu Zhu and Gaoya Dong would also like to acknowledge the financial support from University College Dublin (UCD) and China Scholarship Council (CSC, China) for their PhD study under the UCD-CSC Scholarship scheme.

References

- Arteaga, V. G., Guardia, M. A., Muranyi, I., Eisner, P., & Schweiggert-Weisz, U. (2020). Effect of enzymatic hydrolysis on molecular weight distribution, techno-functional properties and sensory perception of pea protein isolates. *Innovative Food Science & Emerging Technologies*, 65, Article 102449.
- Asaithambi, N., Singha, P., Dwivedi, M., & Singh, S. K. (2019). Hydrodynamic cavitation and its application in food and beverage industry: A review. *Journal of Food Process Engineering*, 42(5), Article e13144.
- Bernardi, S., Lupatini-Menegotto, A. L., Kalschne, D. L., Moraes Flores, É. L., Bittencourt, P. R. S., Colla, E., et al. (2021). Ultrasound: A suitable technology to improve the extraction and techno-functional properties of vegetable food proteins. *Plant Foods for Human Nutrition, 76*, 1–11.
- Bhargava, N., Mor, R. S., Kumar, K., & Sharanagat, V. S. (2021). Advances in application of ultrasound in food processing: A review. *Ultrasonics Sonochemistry*, 70, Article 105293.
- Carvalho, L. B., Capelo-Martínez, J. L., Lodeiro, C., Wiśniewski, J. R., & Santos, H. M. (2019). Snap-heated freeze-free preservation and processing of the urine proteome using the combination of stabilizor-based technology and filter aided sample preparation. *Analytica Chimica Acta*, 1076, 82–90.
- Carvalho, L. B., Capelo-Martinez, J.-L., Lodeiro, C., Wisniewski, J. R., & Santos, H. M. (2020). Ultrasonic-based filter aided sample preparation as the general method to sample preparation in proteomics. *Analytical Chemistry*, 92(13), 9164–9171.
- Cheng, J., & Cui, L. (2021). Effects of high-intensity ultrasound on the structural, optical, mechanical and physicochemical properties of pea protein isolate-based edible film. Ultrasonics Sonochemistry, 80, Article 105809.
- Cox, J., & Mann, M. (2008). MaxQuant enables high peptide identification rates, individualized ppb-range mass accuracies and proteome-wide protein quantification. *Nature Biotechnology*, 26(12), 1367–1372.
- Cox, J., Neuhauser, N., Michalski, A., Scheltema, R. A., Olsen, J. V., & Mann, M. (2011). Andromeda: A peptide search engine integrated into the MaxQuant environment. *Journal of Proteome Research*, 10(4), 1794–1805.
- Das, R. S., Zhu, X., Hannon, S., Mullins, E., Alves, S., Garcia-Vaquero, M., et al. (2023). Exploring Osborne fractionation and laboratory/pilot scale technologies (conventional extraction, ultrasound-assisted extraction, high-pressure processing and hydrodynamic cavitation) for protein extraction from faba bean (Vicia faba L.). Innovative Food Science & Emerging Technologies, 89, Article 103487.
- de Oliveira, A. P. H., Omura, M. H., Barbosa, É.d. A. A., Bressan, G. C., Vieira, É. N. R., dos Reis Coimbra, J. S., et al. (2020). Combined adjustment of pH and ultrasound treatments modify techno-functionalities of pea protein concentrates. Colloids and Surfaces A: Physicochemical and Engineering Aspects, 603, Article 125156.
- Esua, O. J., Cheng, J.-H., & Sun, D.-W. (2021a). Optimisation of treatment conditions for reducing shewanella putrefaciens and salmonella typhimurium on grass carp treated by thermoultrasound-assisted plasma functionalized buffer. *Ultrasonics* Sonochemistry, 76, 105609.
- Esua, O. J., Cheng, J.-H., & Sun, D.-W. (2021b). Novel technique for treating grass carp (Ctenopharyngodon idella) by combining plasma functionalized liquids and ultrasound: effects on bacterial inactivation and quality attributes. *Ultrasonics* Sonochemistry, 76, 105660.
- Esua, O. J., Sun, D.-W., Cheng, J.-H., Wang, H., & Chen, C. (2022). Hybridising plasma functionalized water and ultrasound pretreatment for enzymatic protein hydrolysis of larimichthys polyactis: parametric screening and optimization. Food Chemistry, 385, 132677.
- Esua, O. J., Sun, D.-W., Cheng, J.-H., Wang, H., & Lv, M. (2022). Functional and bioactive properties of larimichthys polyactis protein hydrolysates as influenced by plasma functionalized water-ultrasound hybrid treatments and enzyme types. *Ultrasonics* Sonochemistry, 86, 106023.
- Gao, K., Rao, J., & Chen, B. (2022). Unraveling the mechanism by which high intensity ultrasound improves the solubility of commercial pea protein isolates. *Food Hydrocolloids*, 131, Article 107823.
- Gao, K., Zha, F., Yang, Z., Rao, J., & Chen, B. (2022). Structure characteristics and functionality of water-soluble fraction from high-intensity ultrasound treated pea protein isolate. *Food Hydrocolloids*, 125, Article 107409.
 Kamal, H., Ali, A., Manickam, S., & Le, C. F. (2022). Impact of cavitation on the structure
- Kamal, H., Ali, A., Manickam, S., & Le, C. F. (2022). Impact of cavitation on the structure and functional quality of extracted protein from food sources–An overview. Food Chemistry, Article 135071.

- Karabulut, G., Yildiz, S., Karaca, A. C., & Yemiş, O. (2023). Ultrasound and enzyme-pretreated extraction for the valorization of pea pod proteins. *Journal of Food Process Engineering*, Article e14452.
- Kiani, H., Sun, D.-W., & Zhang, Z. (2012). The effect of ultrasound irradiation on the convective heat transfer rate during immersion cooling of a stationary sphere. *Ultrasonics Sonochemistry*, 19(6), 1238–1245.
- Kiani, H., Sun, D.-W., & Zhang, Z. (2013). Effects of processing parameters on the convective heat transfer rate during ultrasound assisted low temperature immersion treatment of a stationary sphere. *Journal of Food Engineering*, 115(3), 384–390.
- Lam, A., Can Karaca, A., Tyler, R., & Nickerson, M. (2018). Pea protein isolates: Structure, extraction, and functionality. Food Reviews International, 34(2), 126–147.
- Li, C., Yang, F., Huang, Y., Huang, C., Zhang, K., & Yan, L. (2020). Comparison of hydrodynamic and ultrasonic cavitation effects on soy protein isolate functionality. *Journal of Food Engineering*, 265, Article 109697.
- Liu, L., Miao, Y., Hu, C., Gao, L., He, W., Chu, H., et al. (2023). Effect of ultrasonic frequency on the structural and functional properties of pea protein isolation. *Journal of the Science of Food and Agriculture*.
- Moll, P., Salminen, H., Seitz, O., Schmitt, C., & Weiss, J. (2023). Characterization of soluble and insoluble fractions obtained from a commercial pea protein isolate. *Journal of Dispersion Science and Technology*, 44(13), 2417–2428.
- Möller, A. C., van der Padt, A., & van der Goot, A. J. (2021). From raw material to mildly refined ingredient–Linking structure to composition to understand fractionation processes. *Journal of Food Engineering*, 291, Article 110321.
- Mozafarpour, R., Koocheki, A., & Nicolai, T. (2022). Modification of grass pea protein isolate (Lathyrus sativus L.) using high intensity ultrasound treatment: Structure and functional properties. Food Research International, 158, Article 111520.
- Ochoa-Rivas, A., Nava-Valdez, Y., Serna-Saldívar, S. O., & Chuck-Hernández, C. (2017). Microwave and ultrasound to enhance protein extraction from peanut flour under alkaline conditions: Effects in yield and functional properties of protein isolates. Food and Bioprocess Technology, 10(3), 543–555.
- Official methods of analysis of the association of official analytical chemistry (16th ed.). (1995).
- Pernollet, J.-C. (1978). Protein bodies of seeds: Ultrastructure, biochemistry, biosynthesis and degradation. *Phytochemistry*, 17(9), 1473–1480.
- Preece, K., Hooshyar, N., Krijgsman, A., Fryer, P., & Zuidam, N. (2017). Intensification of protein extraction from soybean processing materials using hydrodynamic cavitation. *Innovative Food Science & Emerging Technologies*, 41, 47–55.
- Sahil, Madhumita, M., Prabhakar, P. K., & Kumar, N. (2022). Dynamic high pressure treatments: Current advances on mechanistic-cum-transport phenomena approaches and plant protein functionalization. Critical Reviews in Food Science and Nutrition, 1–26.
- Shen, S., Hou, H., Ding, C., Bing, D.-J., & Lu, Z.-X. (2016). Protein content correlates with starch morphology, composition and physicochemical properties in field peas. *Canadian Journal of Plant Science*, *96*(3), 404–412.
- Shevkani, K., Singh, N., Kaur, A., & Rana, J. C. (2015). Structural and functional characterization of kidney bean and field pea protein isolates: A comparative study. *Food Hydrocolloids*, 43, 679–689.
- Sun, X., You, W., Wu, Y., Tao, Y., Yoon, J. Y., Zhang, X., et al. (2022). Hydrodynamic cavitation: A novel non-thermal liquid food processing technology. Frontiers in Nutrition, 9, Article 843808.
- Swanson, B. G. (1990). Pea and lentil protein extraction and functionality. *Journal of the American Oil Chemists' Society*, 67(5), 276–280.
- Tang, J., Zhu, X., Jambrak, A. R., Sun, D.-W., & Tiwari, B. K. (2023). Mechanistic and synergistic aspects of ultrasonics and hydrodynamic cavitation for food processing. *Critical Reviews in Food Science and Nutrition*, 1–22.
- Tanger, C., Engel, J., & Kulozik, U. (2020). Influence of extraction conditions on the conformational alteration of pea protein extracted from pea flour. *Food Hydrocolloids*, 107, Article 105949.
- Tyanova, S., Temu, T., Carlson, A., Sinitcyn, P., Mann, M., & Cox, J. (2015). Visualization of LC-MS/MS proteomics data in MaxQuant. *Proteomics*, 15(8), 1453–1456.
- Tyanova, S., Temu, T., Sinitcyn, P., Carlson, A., Hein, M. Y., Geiger, T., et al. (2016). The Perseus computational platform for comprehensive analysis of (prote) omics data. *Nature Methods*, 13(9), 731–740.
- Venkateswara Rao, M., CK, S., Rawson, A., DV, C., & N, V. (2023). Modifying the plant proteins techno-functionalities by novel physical processing technologies: A review. *Critical Reviews in Food Science and Nutrition*, 63(19), 4070–4091.
- Wang, B., Su, H., & Zhang, B. (2021). Hydrodynamic cavitation as a promising route for wastewater treatment—A review. Chemical Engineering Journal, 412, Article 128685.
- Wang, F., Zhang, Y., Xu, L., & Ma, H. (2020). An efficient ultrasound-assisted extraction method of pea protein and its effect on protein functional properties and biological activities. Lebensmittel-Wissenschaft und -Technologie, 127, Article 109348.
- Wen, L., Álvarez, C., Zhang, Z., Poojary, M. M., Lund, M. N., Sun, D.-W., & Tiwari, B. K. (2021). Optimization and characterization of protein extraction from coffee silverskin assisted by ultrasound or microwave techniques. *Biomass Conversion and Biorefinery*, 11(5), 1575–1585.
- Wiśniewski, J. R. (2019). Filter aided sample preparation—a tutorial. *Analytica Chimica Acta, 1090*, 23–30.
- Wiśniewski, J. R., Zougman, A., Nagaraj, N., & Mann, M. (2009). Universal sample preparation method for proteome analysis. *Nature Methods*, 6(5), 359–362.
- Xiong, T., Xiong, W., Ge, M., Xia, J., Li, B., & Chen, Y. (2018). Effect of high intensity ultrasound on structure and foaming properties of pea protein isolate, 2018/07/01/ Food Research International, 109, 260–267. https://doi.org/10.1016/j. foodres.2018.04.044.
- Yan, J., Zhao, S., Xu, X., & Liu, F. (2024). Enhancing pea protein isolate functionality: A comparative study of high-pressure homogenization, ultrasonic treatment, and combined processing techniques. Current Research in Food Science, 8, Article 100653.

- Yang, J., Zamani, S., Liang, L., & Chen, L. (2021). Extraction methods significantly impact pea protein composition, structure and gelling properties. Food Hydrocolloids, 117, Article 106678.
- Youshanlouei, Y. A., Kiani, H., Mousavi, M., & Mousavi, Z. E. (2022). Grass pea (Lathyrus sativus L.) protein yield and functionality as affected by extraction method: Alkaline, ultrasound-assisted, and ultrasound pretreatment extraction. *Cereal Chemistry*, 99(4), 931–946.
- Yusoff, I. M., Taher, Z. M., Rahmat, Z., & Chua, L. S. (2022). A review of ultrasound-assisted extraction for plant bioactive compounds: Phenolics, flavonoids, thymols, saponins and proteins. *Food Research International, 111268*.
- Zhang, B., Kang, X., Cheng, Y., Cui, B., & Abd El-Aty, A. (2022a). Impact of high moisture contents on the structure and functional properties of pea protein isolate during extrusion. *Food Hydrocolloids, 127*, Article 107508.
- Zhang, J., Liu, Q., Chen, Q., Sun, F., Liu, H., & Kong, B. (2022b). Synergistic modification of pea protein structure using high-intensity ultrasound and pH-shifting technology

- to improve solubility and emulsification. $Ultrasonics\ Sonochemistry,\ 88,\ Article\ 106099.$
- Zhang, P., Zhu, Z., & Sun, D.-W. (2018). Using power ultrasound to accelerate food freezing processes: effects on freezing efficiency and food microstructure. *Critical Reviews in Food Science and Nutrition*, 58(16), 2842–2853.
- Zhu, Z., Sun, D.-W., Zhang, Z., Li, Y., & Cheng, L. (2018). Effects of micro-nano bubbles on the nucleation and crystal growth of sucrose and maltodextrin solutions during ultrasound-assisted freezing process. LWT - Food Science and Technology, 92, 404–411.
- Zhu, Z., Chen, Z., Zhou, Q., & Sun, D.-W. (2018). Freezing efficiency and quality attributes as affected by voids in plant tissues during ultrasound-assisted immersion freezing. Food and Bioprocess Technology, 11(9), 1615–1626.
- Zhu, X., Healy, L. E., Sevindik, O., Sun, D.-W., Selli, S., Kelebek, H., et al. (2022). Impacts of novel blanching treatments combined with commercial drying methods on the physicochemical properties of Irish brown seaweed Alaria esculenta. *Food Chemistry*, 369, Article 130949.